Cosmic ray Monte Carlo: A global fitting method in studying the properties of the new sources of cosmic $e^{\pm}$ excesses

Jie Liu,[1] Qiang Yuan,[2] Xiao-Jun Bi,[2] Hong Li,[1,3] and Xinmin Zhang[1,3]

[1]*Theoretical Physics Division, Institute of High Energy Physics, Chinese Academy of Science, P.O. Box 918-4, Beijing 100049, People's Republic of China*

[2]*Key Laboratory of Particle Astrophysics, Institute of High Energy Physics, Chinese Academy of Science, P.O. Box 918-3, Beijing 100049, People's Republic of China*

[3]*Theoretical Physics Center for Science Facilities (TPCSF), Chinese Academy of Science, Beijing 100049, People's Republic of China*

(Received 6 August 2011; published 7 February 2012)

Recently, the PAMELA collaboration published the cosmic nuclei and electron spectra with high precision, together with the cosmic antiproton data updated, and the Fermi-LAT collaboration also updated the measurement of the total e^+e^- spectrum to lower energies. In this paper we develop a Markov Chain Monte Carlo (MCMC) package *CosRayMC*, based on the Galactic Propagation (GALPROP) cosmic ray propagation model to study the implications of these new data. It is found that if only the background electrons and secondary positrons are considered, the fit is very bad with $\chi^2_{\rm red} \approx 3.39$. Taking into account the extra e^+e^- sources of pulsars or dark matter annihilation we can give much better fit to these data, with the minimum $\chi^2_{\rm red} \approx 1.04$. This means the extra sources are necessary with a very high significance in order to fit the data. However, the data show little difference between pulsar and dark matter scenarios. Both the background and extra source parameters are well constrained with this MCMC method. The antiproton data can further constrain the branching ratio of dark matter annihilation into quarks to be $B_q < 0.5\%$ at 2σ confidence level. The possible systematical uncertainties of the present study are discussed.

DOI: 10.1103/PhysRevD.85.043507 PACS numbers: 95.35.+d, 96.50.S−

I. INTRODUCTION

A very interesting progress made in recent years in cosmic ray (CR) physics is the discovery of the excesses of positrons and electrons by several space- and ground-based experiments [1–5]. The positron and electron excesses challenge the traditional understanding of CR background. Many theoretical models were proposed to explain these new phenomena, including the astrophysical scenarios (e.g., [6–13], and see [14] for a review) and the dark matter (DM) scenario (e.g., [15–18]).

Most recently, the Fermi-LAT team reported the updated measurements of the total spectrum of electrons and positrons, extending to energies as low as several GeV [19]. PAMELA collaboration updated the observation of the $\bar{p}/p$ ratio and the absolute antiproton flux [20], and reported the measurement of the pure electron spectrum for the first time [21]. The antiproton data extend to 180 GeV, without any hint of deviation from the background contribution [20]. For the PAMELA electron data, although there is no significant spectral feature above 30 GeV other than a single-power law, it is also consistent with models including extra e^+e^- sources to explain the positron excess [21]. There is also hint of hardening of the electron spectrum compared with the low energy part (< 20 GeV), although the solar modulation may be important at these low energies.

Since the accumulation of high-quality CR data, it is now important to extract more information from these data, i.e., estimating the CR background and the possible extra source parameters. Previously, one always constrained one or two parameters with other parameters fixed. This may lead to biased results, especially when the parameters are strongly correlated. The global fitting procedure searches the maximum likelihood in the multiple dimensional parameter space rather than a reduced one and can give the posterior distribution by marginalizing other parameters in the Bayesian approach. The Markov Chain Monte Carlo (MCMC) procedure, whose computational time scales approximately linearly with the number of parameters, makes it possible to survey in a very large parameter space with the least computational cost.

In our previous studies [22,23], we employed the MCMC method to fit the parameters of the DM scenario as well as the background parameters proposed to explain the e^+e^- excesses. However, the propagation of CRs is treated with a semianalytical way following Refs. . A more precise description of the CR propagation is given by the numerical models, such as GALPROP and DRAGON , in which most of the relevant physical processes are taken into account, and the realistic astrophysical inputs like the interstellar medium (ISM) and the interstellar radiation field (ISRF) are adopted. There are many parameters in the CR propagation model, and it is very difficult to have a full and systematical survey of the parameter space. After embedding the numerical CR propagation tool into the MCMC sampler, we can use it to constrain the model parameters in a more efficient way. Recently there are

also several other works using the MCMC method to study the CR propagation [29–31].

In this work, we develop a package *CosRayMC* (Cosmic Ray MCMC), which is comprised of GALPROP, PYTHIA [32] and MCMC sampler, to revisit the models to explain the positron and electron excesses and derive the constraints on the model parameters with the latest data. Two kinds of the extra e^+e^- sources are considered: the pulsar scenario and the DM annihilation scenario. In both scenarios we consider the continuous distribution of the sources, although it is possible that one or several nearby pulsars or DM subhalos may explain the excesses [6,7,33–35]. As pointed out in [36], it was unlikely that the flux from any single pulsar was significantly larger than that from others given a large number of known nearby and energetic pulsars. For DM subhalos the location and mass are uncertain, which also makes the constraints of the model parameters difficult.

This paper is organized as follows. We briefly introduce the propagation of Galactic CRs in Sec. II. The description of the methodology is given in Sec. III. The fitting results of the pulsar and DM scenarios are presented in Sec. IV. Finally we give the conclusion and discussion in Sec. V.

II. PROPAGATION OF GALACTIC COSMIC RAYS

The charged particles propagate diffusively in the Galaxy due to the scattering with random magnetic field. There are interactions between the CR particles and the ISM and/or the ISRF, which will lead to fragmentation, catastrophic or continuous energy losses of the particles. For unstable nuclei the radioactive decay also needs to be taken into account. In addition, the overall convection driven by the stellar wind and reacceleration due to the interstellar shock will also affect the distribution function of CRs. For each species of particles we have a partial differential equation to describe the propagation process, with the general form [37]

$$\frac{\partial \psi}{\partial t} = Q(\mathbf{x}, p) + \nabla \cdot (D_{xx}\nabla\psi - \mathbf{V_c}\psi) + \frac{\partial}{\partial p} p^2 D_{pp} \frac{\partial}{\partial p} \frac{1}{p^2}\psi - \frac{\partial}{\partial p}\left[\dot{p}\psi - \frac{p}{3}(\nabla \cdot \mathbf{V_c}\psi)\right] - \frac{\psi}{\tau_f} - \frac{\psi}{\tau_r}, \quad (1)$$

where ψ is the density of cosmic ray particles per unit momentum interval, $Q(\mathbf{x}, p)$ is the source term, D_{xx} is the spatial diffusion coefficient, $\mathbf{V_c}$ is the convection velocity, D_{pp} is the diffusion coefficient in momentum space used to describe the reacceleration process, $\dot{p} \equiv dp/dt$ is the momentum loss rate, τ_f and τ_r are time scales for fragmentation and radioactive decay, respectively. Solving the partially coupled equations for all kinds of particles, we can get the propagated results of the CR spectra and spatial distributions. For more details about the terms in Eq. (1) please refer to the recent review paper [37].

The secondary-to-primary ratios such as B/C and (Sc + Ti + V)/Fe, and the unstable-to-stable ratios of secondary particles such as ^{10}Be/^{9}Be and ^{26}Al/^{27}Al, are often used to constrain the propagation parameters because the ratios can effectively avoid the source parameters. Then one can use the spectra of the primary particles to derive the source parameters. There are some studies to constrain the propagation parameters based on the currently available data (e.g., [27,38,39]). In [29–31] the MCMC method was adopted to fit both the propagation and source parameters of CRs. However, due to the quality of the observational data, the constraints on the propagation parameters are not very effective, and there may be also large systematic uncertainties.

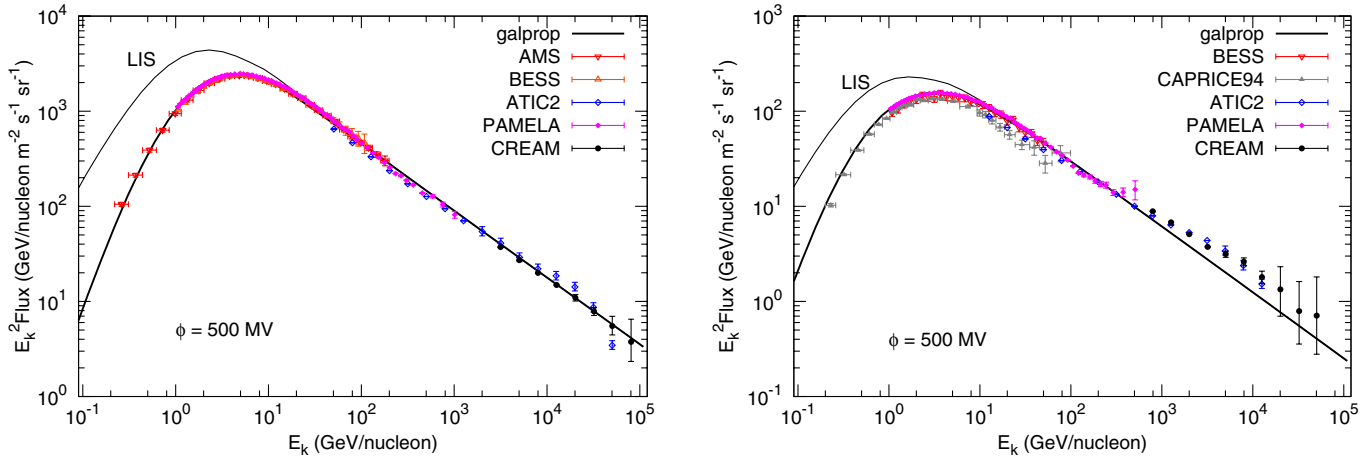

FIG. 1 (color online). Proton (left) and Helium (right) spectra of the GALPROP model calculation, compared with the observational data. In each panel the higher line labeled "LIS" represents the local interstellar flux, and the lower one is the flux after the solar modulation. References of the data are: proton—AMS [75], BESS [76], ATIC2 [77], PAMELA [42], CREAM [41]; Helium—BESS [76], CAPRICE94 [78], ATIC2 [77], PAMELA [42], CREAM [41].

Since we focus on the electron and positron data in this work, which are not very effective to constrain the propagation parameters, we adopt the best fitting results of the propagation parameters given in [31]. The main propagation parameters are: $D_0 = 6.59 \times 10^{28}$ cm^2 s^{-1}, $\delta = 0.30$, $v_A = 39.2$ km s^{-1}, $z_h = 3.9$ kpc. The injection spectra of nuclei are adopted as $\gamma_1^n = 1.91$ (below 10 GV) and $\gamma_2^n = 2.40$ (above 10 GV). What we should keep in mind is that there might be systematic errors of the determination of the propagation parameters (see e.g., [40]), and the quantitative results of this work might be affected.

We note that the newest measurements of the CR proton and Helium spectra by CREAM [41] and PAMELA [42] showed remarkable deviation of single power-law spectra. Furthermore, the spectral indices of proton and Helium are different. Such new features challenge the traditional understanding of the CR origin, acceleration, and propagation (see e.g. [43,44] for some explanations). In the present work we keep the study in the traditional frame and do not try to reproduce the detailed structures of the data. We find that the above adopted injection parameters with proper adjusting of the normalization can basically reproduce the PAMELA-CREAM proton data, as shown in the left panel of Fig. 1. However, when comparing with the Helium data, the model expectation seems to be systematically lower. We increase the relative abundance of Helium in GALPROP by 30%, and give a roughly consistent result with the PAMELA data (right panel of Fig. 1). The CREAM data can still not be reproduced. Since the contribution to the secondary particles from CR Helium is only a small fraction, we do not think a higher Helium flux within a factor of 2 will substantially affect our following study. Actually, we have checked that taking $\gamma_1^{\rm He} = 1.96$, $\gamma_2^{\rm He} = 2.35$ can give a rough description to the CREAM data of Helium. In this case the change of the secondary positrons (antiprotons) is less than 5% at 100 GeV.

III. METHODOLOGY

A. CosRayMC

The *CosRayMC* (Cosmic Ray MCMC) code is built up by embedding the CR propagation code GALPROP (v51) into the MCMC sampling scheme. The MCMC technique is widely applied to give multidimensional parameter constraints from observational data. Following Bayes' Theorem, the posterior probability of a model (which we refer to a series of parameters $\vec{\theta}$) given the data (which are described by D) is

$$\mathcal{P}(\vec{\theta}|D) \propto \mathcal{L}(\vec{\theta})\mathcal{P}(\vec{\theta}), \tag{2}$$

where $\mathcal{L}(\vec{\theta}) = P(D|\vec{\theta})$ is the likelihood function of the model $\vec{\theta}$ for the data D, and $\mathcal{P}(\vec{\theta})$ is the prior probability of the model parameters. In performing *CosRayMC*, MCMC is employed to generate a random sample from the posterior distribution $\mathcal{P}(\vec{\theta}|D)$ which are fair samples of the likelihood surface. Based on the sample, we can get the estimate of the mean values, the variance as well as the confidence level of the model parameters. For details please refer to [45].

The key improvement, compared with our previous study, is that the calculation of the likelihood $\mathcal{L}(\vec{\theta})$ are given by calling GALPROP to simulate the mock observations. By doing so, we can have a more precise description of the CR propagation. And as the better data set is provided in the future, our code can also be used to make a determination of the CR propagation parameters.

For the part with DM contribution to the CRs, the PYTHIA (v6.4) simulation code is employed to calculate the final spectra of electrons, positrons and antiprotons [32]. Such spectra are then injected into the Galaxy and propagated with GALPROP. The PYTHIA code is also embedded in the *CosRayMC* code.

B. Parameters

We assume the injection spectrum of the background electrons to be a broken power-law function with spectral indices γ_1/γ_2 below/above $E_{\rm br}$. Note that for the shock acceleration scenario, the injection spectrum of particles can not be too hard [46]. We set the priors that $\gamma_1 > 1.5$ and $\gamma_2 > 1.5$ in the MCMC scanning. The normalization of background electrons $A_{\rm bkg}$, taken as the flux of electrons at 25 GeV, is also regarded as a free parameter. For the background positrons and antiprotons, we adopt the GALPROP model predicted results with the best fitting source and propagation parameters given in [31]. Considering the fact that there are uncertainties about the ISM density distribution, the hadronic interaction model, and the propagation parameters determined from the secondary-to-primary ratio data, we will further employ factors c_{e^+} and $c_{\bar{p}}$ to rescale the absolute fluxes of the secondary positrons/electrons and antiprotons.

For energies below $\sim$30 GeV the solar modulation effect is important and needs to be considered. In this work we adopt the force-field approximation to calculate the solar modulation [47]. The modulation potential depends on the solar activity. For the period which PAMELA works the modulation potential is estimated to be $\phi =$ 450–550 MV [42]. However, the determination of the modulation parameter will depend on the choices of the interstellar spectra, and can not be precisely figured out. In our MCMC fit, we take the modulation potential ϕ as a free parameter in the range 300–700 MV, which is an enlarged region based on the preferred one 450–550 MV. Thus, for the background model we have 7 parameters in total:

$$\mathcal{P}_{\rm bkg} = \{\gamma_1, \gamma_2, E_{\rm br}, A_{\rm bkg}, \phi, c_{e^+}, c_{\bar{p}}\}. \tag{3}$$

Pulsars are thought to be the most natural candidates to generate high energy positrons and electrons through the cascade of electrons accelerated in the magnetosphere [33,48]. The spectrum of e^+e^- escaped from the pulsars

can be parameterized as power-law with a cutoff at E_c, $dN/dE \propto A_{\rm psr} E^{-\alpha} \exp(-E/E_c)$, where the power-law index α ranges from 1 to 2.2 according to the radio and gamma-ray observations [33]. The cutoff energy of the injected e^+e^- ranges from several tens GeV to higher than TeV, depending on the models and parameters of the pulsars [36,48]. For the spatial distribution of pulsars, we adopt the following form [49]:

$$f(R, z) \propto \left(\frac{R}{R_\odot}\right)^a \exp\left[-\frac{b(R-R_\odot)}{R_\odot}\right] \exp\left(-\frac{|z|}{z_s}\right), \quad (4)$$

where $R_\odot = 8.5$ kpc is the distance of solar system from the Galactic center, $z_s \approx 0.2$ kpc is the scale height of the pulsar distribution, $a = 2.35$ and $b = 5.56$. There will be a further normalization factor $A_{\rm psr}$.

Alternatively, DM annihilation or decay models are widely employed to explain the e^+e^- excesses. Since to date one can not distinguish DM annihilation from decay with the e^+e^- data [22,23], we only consider the annihilation scenario here. Considering the nonexcess of PAMELA antiproton data, the DM annihilation final states need to be lepton-dominated [17,18]. Similar as the previous works [22,23], we do not employ the annihilation final states based on any DM models, but to constrain the final states from the data we use a model-independent way instead. Such constraints will be helpful for the understanding of the DM particle nature.

The annihilation final states are assumed to be two-body e^+e^-, $\mu^+\mu^-$, $\tau^+\tau^-$ and $q\bar{q}$,[1] with branching ratios B_e, B_μ, B_τ and B_q, respectively. It was also shown that the interactions with low-mass intermediate bosons, which then decay to lepton pairs, could fit the CR e^+e^- data well [50,51]. However, since the spectral shapes of the electrons and positrons from these models do not have distinct properties which can be easily distinguished from $\mu^+\mu^-$ and $\tau^+\tau^-$, we do not include such final states in this study. The resulting positron, electron and antiproton spectra of these final states are calculated using the PYTHIA simulation package [32].

The DM density profile is assumed to be an Einasto type [52]

$$\rho(r) = \rho_{-2} \exp\left[-\frac{2}{\alpha}\left(\frac{r^\alpha}{r_{-2}^\alpha} - 1\right)\right], \quad (5)$$

where $\alpha \approx 0.17$, $r_{-2} \approx 15.6$ kpc and $\rho_{-2} \approx 0.14\ {\rm GeV\,cm^{-3}}$ according to the recent high resolution simulation *Aquarius* [53]. The corresponding local density of DM is about $0.44\ {\rm GeV\,cm^{-3}}$, which is consistent with the results of a larger local density derived in recent studies [54–56]. Then the source function of positron produced from DM annihilation is

$$q(E, r) = \frac{\langle\sigma v\rangle}{2m_\chi^2} \sum_f B_f \left.\frac{dN}{dE}\right|_f \times \rho^2(r), \quad (6)$$

where m_χ is the mass of the DM particle, $\langle\sigma v\rangle$ is the velocity weighted annihilation cross section, and $\frac{dN}{dE}|_f$ is the positron production rate from channel f of one annihilation.

The most general parameter space is summarized as below:

$$\mathcal{P}_{\rm tol} = \begin{cases} \{\mathcal{P}_{\rm bkg}\}, & \text{background} \\ \{\mathcal{P}_{\rm bkg}, A_{\rm psr}, \alpha, E_c\}, & \text{pulsar} \\ \{\mathcal{P}_{\rm bkg}, m_\chi, \langle\sigma v\rangle, B_e, B_\mu, B_\tau, B_u\}, & \text{DM.} \end{cases} \quad (7)$$

IV. RESULTS

A. Background

First, we run a fit for the pure background contribution. The data included in the fit are: PAMELA positron fraction [1], PAMELA electron [21], Fermi-LAT total e^+e^- [19], and HESS total e^+e^- [3,4]. Both the systematic and statistical uncertainties reported by these experiments are taken into account. For the Fermi-LAT and HESS data of the total e^+e^- fluxes, systematic uncertainties of the absolute energy calibration are translated to the relative uncertainties of the fluxes, which are $(\Gamma - 1)\Delta E/E$ with Γ the spectrum index and $\Delta E/E$ the energy resolution [19].

For the PAMELA positron fraction data, we only employ the data points with $E > 5$ GeV in the fit. For the lower energy part we can see that the PAMELA data are inconsistent with the previous measurements. This may be due to more complicated solar modulation effect or even the charge dependent modulation [57–60]. It was shown that either a model with different modulation potentials for positive and negative charged particle [59] or a detailed Monte Carlo approach to solve the stochastic differential equations of the e^+e^- motion [60] can give consistent description to the PAMELA and previous data. The demodulated interstellar spectra of electrons and positrons are also consistent with the conventional CR background model expectation. Here we do not consider the detailed solar modulation models. But, note that the solar modulation model may affect the quantitative fitting results. This is one kind of systematical errors.

The best-fit results of the positron fraction and electron (or e^+e^-) spectra are shown in Fig. 2. The best-fit parameters are compiled in Table I, with the minimum $\chi^2_{\rm red} \approx 461.0/136 = 3.39$. Such a large reduced χ^2 means that the fit is far from acceptable but systematics dominated. Using

[1]Since the antiproton productions of various quark flavors do not differ much from each other, here we do not distinguish quark flavors but adopt $u\bar{u}$ channel as a typical one of quark final states.

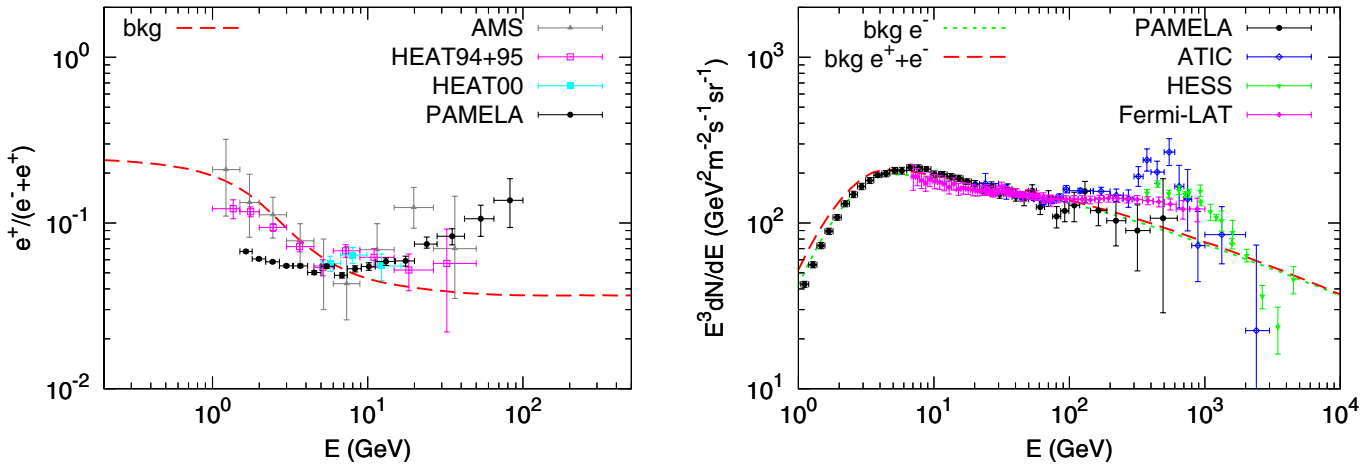

FIG. 2 (color online). Best-fit positron fraction (left) and electron spectra (right) of the pure background case. Note that in the right panel the PAMELA data are for pure electrons, while other data are for the sum of electrons and positrons. References of the observational data are: positron fraction—AMS [79], HEAT94 + 95 [80], HEAT00 [81], PAMELA [1]; electron—PAMELA [21], ATIC [2], HESS [3,4], Fermi-LAT [19].

a χ^2 goodness-of-fit test we find that the background only case is rejected with a very high significance $\sim 20\sigma$. That is to say the data strongly favor the existence of additional degrees of freedom. From Fig. 2 we can clearly see that the background model underestimates both the positron fraction and the total e^+e^- fluxes. The extra sources of e^+e^- are necessary to explain simultaneously the positron fraction and total e^+e^- data.

The poor fit makes nonsense to discuss the physical implication of the parameters. Therefore, we leave the discussion of the parameters in the next subsections, when the extra sources of e^+e^- are taken into account.

B. Pulsar scenario

Next, we add the pulsars as the extra sources of e^+e^-. The fitting parameters are listed in Table I. We find that γ_1 is consistent with 1.60 as that derived in the conventional GALPROP background model [61]. Note that there is a correlation between parameters γ_1 and the modulation potential ϕ, as shown in Fig. 3. The high energy injection spectrum $\gamma_2 = 2.712 \pm 0.014$ is softer than 2.54 as adopted in the conventional model [61]. In the conventional model only the background contribution is employed to fit the data, while here an additional component from the extra sources are added together. Thus, the high energy

TABLE I. Fitting parameters with 1σ uncertainties or 2σ limits. Note that for the "bkg" case the reduced χ^2 is too large that the uncertainties of the parameters should not be statistically meaningful.

	bkg	bkg + pulsar	bkg + DM
γ_1	<1.532 (95% C.L.)	<1.619 (95% C.L.)	<1.610 (95% C.L.)
γ_2	2.557 ± 0.007	2.712 ± 0.014	2.706 ± 0.013
$\log(A_{\rm bkg})$[a]	-8.959 ± 0.003	-8.997 ± 0.007	-8.997 ± 0.006
$E_{\rm br}$ (GeV)	$3.599^{+0.123}_{-0.112}$	$4.254^{+0.278}_{-0.287}$	$4.283^{+0.246}_{-0.259}$
ϕ (GV)	0.324 ± 0.016	0.383 ± 0.042	0.371 ± 0.037
c_{e^+}	1.462 ± 0.035	$1.438^{+0.076}_{-0.079}$	1.394 ± 0.053
$c_{\bar{p}}$	1.194 ± 0.039	1.225 ± 0.043	1.210 ± 0.045
$\log(A_{\rm psr})$[a]	–	$-27.923^{+0.534}_{-0.537}$	–
α	–	1.284 ± 0.104	–
E_c (TeV)	–	$0.861^{+0.170}_{-0.164}$	–
m_χ (TeV)	–	–	$2.341^{+0.492}_{-0.391}$
$\log[\sigma v(\mathrm{cm^3\,s^{-1}})]$	–	–	-22.34 ± 0.13
B_e	–	–	<0.379 (95% C.L.)
B_μ	–	–	<0.334 (95% C.L.)
B_τ	–	–	$0.713^{+0.141}_{-0.152}$
B_u	–	–	<0.005 (95% C.L.)
χ^2/d.o.f	3.390	1.047	1.078

[a]In unit of $\mathrm{cm^{-2}\,sr^{-1}\,s^{-1}\,MeV^{-1}}$.

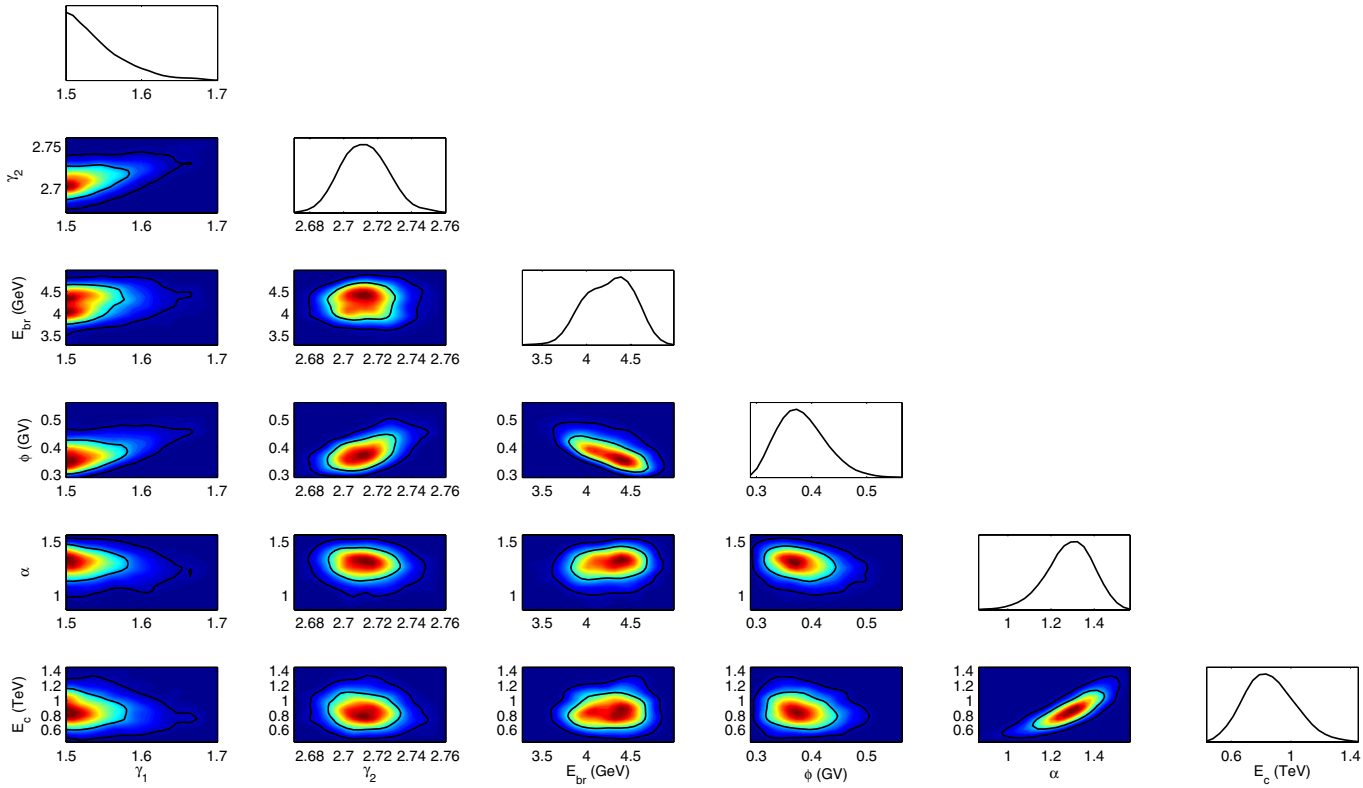

FIG. 3 (color online). Two dimensional constraints of part of the model parameters for the pulsar scenario. In off-diagonal panels, the inner contour denotes the 68% confidence level (C. L.) and the outer contour stands for 95% C. L. The diagonal ones are the marginalized one dimensional probability distributions of the corresponding parameters.

spectrum can be much softer. This might be important for the understanding of the background contribution to the CR electrons.

There is a factor $c_{e^+} \approx 1.4$ needed for the background secondary positrons (same for secondary electrons) to fit the data. As discussed above, such a factor may be ascribed to the uncertainties of the propagation parameters, the ISM density and the strong interaction cross sections. Those uncertainties may be energy-dependent and can not be simply described with a constant factor (see e.g., [8]). For example, in this work we use the parameterization given in [62] (Kamae06) to calculate the pp interaction to generate positrons. Compared with the pp collision model Badhwar77 [63] as adopted in GALPROP, the Kamae06 model gives systematically fewer positrons, especially for energies from several to tens of GeV [8]. If

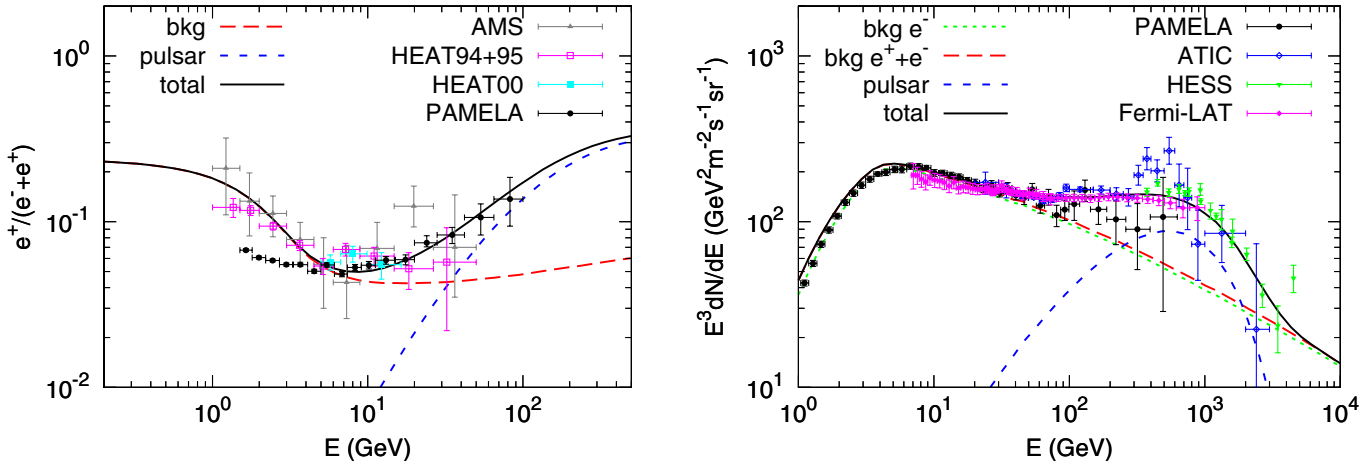

FIG. 4 (color online). Same as Fig. 2 but for the model with pulsars as the extra sources of e^+e^-.

these input uncertainties are better understood in the future, we can include the background positron production with a more general form in the MCMC fit.

The fitted parameters for pulsars are $\alpha = 1.284 \pm 0.104$, $E_c = 0.861^{+0.170}_{-0.164}$ TeV. The constraints of the pulsar parameters are weaker when compared with the background parameters. This is because the cutoff energy is mainly determined by HESS data. However, for HESS data, the very large systematic errors due to poor absolute energy calibration (not shown in Fig. 4) makes it difficult to precisely determine E_c. As discussed in Sec. IVA, a $\sim$15% uncertainty of the energy scale will lead to a flux uncertainty of $\sim$30% and $\sim$45% for energies below and above $\sim$1 TeV. Because of the correlations between E_c and α, $A_{\rm psr}$, the other two parameters are also relatively less constrained.

C. Dark matter annihilation scenario

In this subsection we consider DM annihilation as the extra source of e^+e^- and $\bar{p}$. The fitting parameters are also shown in Table I, and part of the two dimensional confidence regions of the model parameters are presented in Fig. 5. From Table I we find that the background parameters are similar with the pulsar scenario. The overall best-fit χ^2 value of the DM scenario is about 146.7, which is very close to $\chi^2_{\rm psr} \approx 142.4$. That is to say both the astrophysical scenario and DM scenario can give comparable fit to the e^+e^- data. We may not be able to discriminate these two scenarios from the e^+e^- spectra [36,64–67], but need to resort to other probes such as the e^+e^- anisotropy [68] and γ-rays [69].

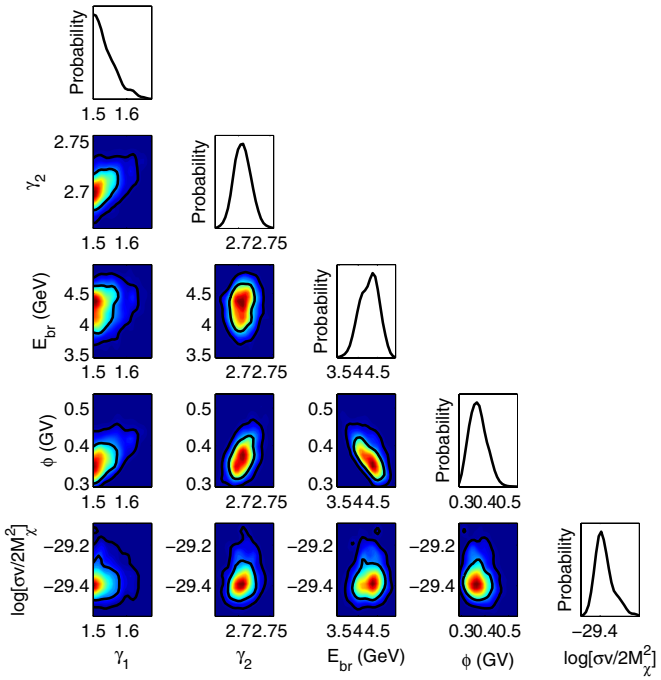

FIG. 5 (color online). Same as Fig. 3 but for the DM annihilation scenario.

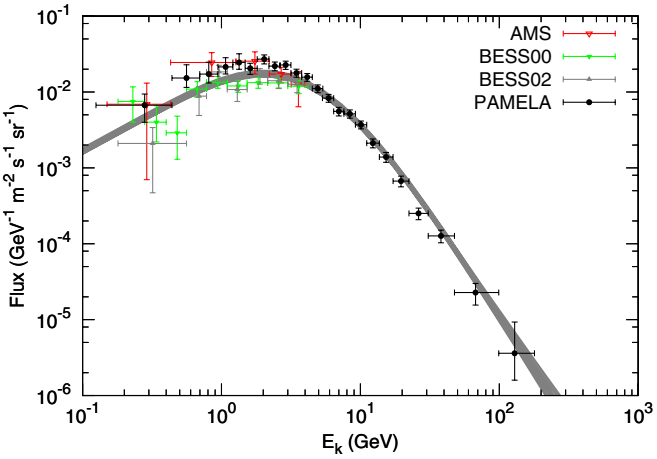

FIG. 6 (color online). Fitted 2σ range of the antiproton fluxes of the DM annihilation scenario. References of the data are: AMS [82], BESS00 [83], BESS02 [84], PAMELA [20].

The fitted mass and cross section of DM are $m_\chi = 2.341^{+0.492}_{-0.391}$ TeV, $\langle\sigma v\rangle = 4.6^{+1.6}_{-1.2} \times 10^{-23}$ cm^3 s^{-1}. Similar to the pulsar case, these parameters are also less constrained due to the large uncertainties of the HESS data. The branch ratio of each channel for dark matter annihilation is $B_e(2\sigma) < 0.38$, $B_\mu(2\sigma) < 0.33$, $B_\tau = 0.69^{+0.14}_{-0.15}$, and $B_u(2\sigma) < 0.5\%$. We should be cautious that the determination of the branching ratios may suffer from systematic uncertainties of the background electrons and positrons. As discussed in the previous subsection, the present understanding of the background positrons is far from precise. Therefore the quoted fitting uncertainties of the branching ratios may be underestimated.

Compared with our previous study [23], the upper limit of B_u is several times smaller. This is probably due to the bad fit to the antiproton data with the current background model. The 2σ range of the antiproton flux is shown in Fig. 6. We can see that the calculated secondary (including tertiary) antiprotons are basically consistent with the PAMELA data for energies higher than several GeV, but underestimate the flux for the low energy part. This problem was pointed out years ago [70,71], that in the diffusive reacceleration model which gives the best fit to the B/C data the antiprotons are underestimated. There seems to be a contradiction between the B/C and the antiproton data.[2]

[2]Note, however, in [72] the calculated antiproton flux based on the propagation parameters fitted according to the B/C data [38] was consistent with the observational data. As pointed out in [71] the fit in [38] was actually based on the high energy data. And in their results the low energy B/C was in fact over estimated. Furthermore the antiproton production cross sections would also lead to uncertainties [71]. Alternatively, in [73] a unified model to explain the B/C and antiproton data was proposed, with an empirical modification of the diffusion coefficient at low speed of particles.

To better understand this issue we may need more precise measurement about the B/C data. Back to this work, a lower antiproton flux at low energies will require a smaller solar modulation potential, and therefore the background parameters γ_1, γ_2 and $E_{\rm br}$ will change accordingly due to the correlations among them as shown in Fig. 5.

We have run a test to employ the background antiproton spectrum used in [23] and found that the 2σ upper limit of B_u is about 2.1%, which is consistent with the previous results. This means that the current constraint on B_u is systematics dominated. Better understanding of the background contribution to the antiproton flux is necessary to further address this issue.

V. CONCLUSION AND DISCUSSION

Recently more and more observational data of CRs with unprecedented precision are available, which makes it possible to better approach the understanding of the basic problems of CRs. Based on MCMC analysis in our previous work [22,23], we embed GALPROP and PYTHIA into MCMC sampler and study the implication of the newest CR data, including the positron fraction, electrons (pure e^- and e^+e^-) and antiprotons from PAMELA, Fermi-LAT and HESS experiments in this work.

We work in the frame of diffusive reacceleration propagation model of CRs. The propagation parameters are adopted according to the fit to currently available B/C data [31], with a slight adjustment of the Helium abundance to better match the PAMELA data [42]. We find that the pure background to explain the CR e^+e^- data is disfavored with a very high significance. Therefore, it is strongly implied that we may need some extra sources to produce the positrons/electrons.

We then consider two different scenarios, which are widely discussed in recent literature, to explain the e^+e^- excesses. One is the astrophysical scenario with pulsars as the typical example, and the other is the DM annihilation scenario. Using the global fitting method, we can determine the parameters of both the background and the extra sources. The low energy spectral index of the background electrons is consistent with the conventional model adopted in the previous study, while the high energy index is softer in this work. We find that, together with the background contribution, both of these scenarios can give very good fit to the data. And the branching ratio to quarks of the DM annihilation final states is constrained to be $<0.5\%$ at 2σ confidence level.

The constraint on the quark branching ratio (or the cross section to quarks) allows us to make a comparison with the direct detection experiments, assuming some effective interaction operators between DM and standard model (SM) particles. As shown in [74], generally the constraint of DM-SM coupling from direct experiments is much stronger than the indirect search for spin-independent interactions. However, for the spin-dependent interactions, the indirect search constraint could be comparable or stronger than the direct experiments. In Fig. 7 we give the constraints on the spin-dependent DM-neutron scattering cross section according to the cross section of DM annihilation to quarks, assuming the axial vector interaction form of DM particles and SM fermions. The ratio between $\langle\sigma v\rangle$ and $\sigma^{\rm SD}_{\chi n}$ is $5c(1+m_n/m_\chi)^2/m_n^2 \times \sum_q \sqrt{1-m_q^2/m_\chi^2}\, m_q^2$ [74], where c is light speed, m_n is the mass of neutron and m_q is the mass of quark. The sum is for all the flavors of quarks. Considering the uncertainties of the background antiprotons, we show the results of two antiproton background models with shaded region: the result calculated in this work and the one used in [23]. The results show that the constraint on the spin-dependent cross section between DM and nucleon from PAMELA antiproton data is much stronger than the direct experiments.

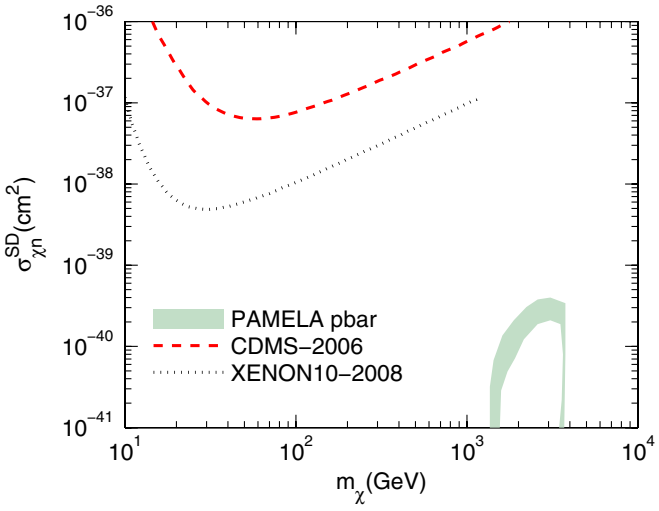

FIG. 7 (color online). Constraints on the spin-dependent DM-neutron scattering cross section from the PAMELA antiproton data assuming axial vector interaction form of DM particles and SM fermions. The shaded region represents the uncertainties of the astrophysical background of antiprotons. Also shown are the results from CDMS [85] and XENON10 [86].

Although the existence of the extra sources is evident, we still can not discriminate the pulsar and DM scenarios right now. These two models both can fit the data very well, with $\chi^2_{\rm red}=1.047$ and $\chi^2_{\rm red}=1.078$, respectively. Other new probes such as the e^+e^- anisotropy and γ-rays are needed to distinguish these models.

The γ-rays should give further constraints on the models, especially for the DM annihilation scenario. However, the diffuse γ-ray data of Fermi-LAT are still in processing, and the modeling of the γ-ray data seems not trivial. Furthermore, the γ-rays are more sensitive to the density profile of DM, which is not the most relevant parameter of the present study. Therefore we do not include the γ-ray

data. It should be a future direction to include the γ-ray data in the *CosRayMC* package.

There are some systematical uncertainties of the current study, which are mainly due to the lack of knowledge about the related issues and can be improved in the future. First, the solar modulation which affects the low energy spectra of CR particles ($E \lesssim 30$ GeV) if not clear. In this work we use the simple force-field approximation [47] to deal with the solar modulation. But such a model seems to fail to explain the low energy data of the PAMELA positron fraction, which may indicate the charge dependent modulation effect [57,59,60]. Second, the propagation model is adopted as the diffusive reacceleration model with the parameters best fitting the B/C data [31]. There are uncertainties of the propagation parameters. Furthermore, the diffusive reacceleration model may also have some systematical errors when comparing with all of the CR data. For example, the antiprotons below several GeV are underestimated in this model. We need to understand the propagation model better with more precise data. Third, the secondary positron and antiproton production may suffer from the uncertainties from the ISM distribution and the hadronic cross sections. All of these uncertainties may affect the quantitative results of the current study. Nevertheless, with more and more precise data available in the near future (e.g., AMS02, which was launched recently), and better control of the above mentioned systematical errors, it is a right direction to do the global fit to derive the constraints and implication on the models.

ACKNOWLEDGMENTS

We thank Hong-Bo Hu and Zhao-Huan Yu for helpful discussions. The calculation is taken on Deepcomp7000 of Supercomputing Center, Computer Network Information Center of the Chinese Academy of Sciences. This work is supported in part by National Natural Science Foundation of China under Grant Nos. 90303004, 10533010, 10675136, 10803001, 11033005, and 11075169, by the 973 Program under Grant No. 2010CB83300, by the Chinese Academy of Science under Grant No. KJCX2-EW-W01, and by the Youth Foundation of the Institute of High Energy Physics under Grant No. H95461N.

[1] O. Adriani, G. C. Barbarino, G. A. Bazilevskaya, R. Bellotti, M. Boezio, E. A. Bogomolov, L. Bonechi, M. Bongi, V. Bonvicini, S. Bottai *et al.*, Nature (London) **458**, 607 (2009).
[2] J. Chang, J. H. Adams, H. S. Ahn, G. L. Bashindzhagyan, M. Christl, O. Ganel, T. G. Guzik, J. Isbert, K. C. Kim, E. N. Kuznetsov *et al.*, Nature (London) **456**, 362 (2008).
[3] F. Aharonian, A. G. Akhperjanian, U. Barres de Almeida, A. R. Bazer-Bachi, Y. Becherini, B. Behera, W. Benbow, K. Bernlöhr, C. Boisson, A. Bochow *et al.*, Phys. Rev. Lett. **101**, 261104 (2008).
[4] F. Aharonian, A. G. Akhperjanian, G. Anton, U. Barres de Almeida, A. R. Bazer-Bachi, Y. Becherini, B. Behera, K. Bernlöhr, A. Bochow, C. Boisson *et al.*, Astron. Astrophys. **508**, 561 (2009).
[5] A. A. Abdo, M. Ackermann, M. Ajello, W. B. Atwood, M. Axelsson, L. Baldini, J. Ballet, G. Barbiellini, D. Bastieri, M. Battelino *et al.*, Phys. Rev. Lett. **102**, 181101 (2009).
[6] H. Yüksel, M. D. Kistler, and T. Stanev, Phys. Rev. Lett. **103**, 051101 (2009).
[7] D. Hooper, P. Blasi, and P. Dario Serpico, J. Cosmol. Astropart. Phys. 1 (2009) 025.
[8] T. Delahaye, R. Lineros, F. Donato, N. Fornengo, J. Lavalle, P. Salati, and R. Taillet, Astron. Astrophys. **501**, 821 (2009).
[9] H.-B. Hu, Q. Yuan, B. Wang, C. Fan, J.-L. Zhang, and X.-J. Bi, Astrophys. J. Lett. **700**, L170 (2009).
[10] N. J. Shaviv, E. Nakar, and T. Piran, Phys. Rev. Lett. **103**, 111302 (2009).
[11] P. Blasi, Phys. Rev. Lett. **103**, 051104 (2009).
[12] D. Grasso *et al.* (FERMI-LAT Collaboration), Astropart. Phys. **32**, 140 (2009).
[13] M. Ahlers, P. Mertsch, and S. Sarkar, Phys. Rev. D **80**, 123017 (2009).
[14] Y.-Z. Fan, B. Zhang, and J. Chang, Int. J. Mod. Phys. D **19**, 2011 (2010).
[15] L. Bergström, T. Bringmann, and J. Edsjö, Phys. Rev. D **78**, 103520 (2008).
[16] V. Barger, W.-Y. Keung, D. Marfatia, and G. Shaughnessy, Phys. Lett. B **672**, 141 (2009).
[17] M. Cirelli, M. Kadastik, M. Raidal, and A. Strumia, Nucl. Phys. **B813**, 1 (2009).
[18] P. F. Yin, Q. Yuan, J. Liu, J. Zhang, X. J. Bi, S. H. Zhu, and X. M. Zhang, Phys. Rev. D **79**, 023512 (2009).
[19] M. Ackermann, M. Ajello, W. B. Atwood, L. Baldini, J. Ballet, G. Barbiellini, D. Bastieri, B. M. Baughman, K. Bechtol, F. Bellardi *et al.*, Phys. Rev. D **82**, 092004 (2010).
[20] O. Adriani, G. C. Barbarino, G. A. Bazilevskaya, R. Bellotti, M. Boezio, E. A. Bogomolov, L. Bonechi, M. Bongi, V. Bonvicini, S. Borisov *et al.*, Phys. Rev. Lett. **105**, 121101 (2010).
[21] O. Adriani, G. C. Barbarino, G. A. Bazilevskaya, R. Bellotti, M. Boezio, E. A. Bogomolov, M. Bongi, V. Bonvicini, S. Borisov, S. Bottai *et al.*, Phys. Rev. Lett. **106**, 201101 (2011).
[22] J. Liu, Q. Yuan, X. Bi, H. Li, and X. Zhang, Phys. Rev. D **81**, 023516 (2010).
[23] J. Liu, Q. Yuan, X. J. Bi, H. Li, and X. M. Zhang, arXiv:0911.1002.
[24] J. Lavalle, Q. Yuan, D. Maurin, and X. Bi, Astron. Astrophys. **479**, 427 (2008).

[25] J. Lavalle, J. Pochon, P. Salati, and R. Taillet, Astron. Astrophys. **462**, 827 (2007).
[26] D. Maurin, R. Taillet, and C. Combet, arXiv:astro-ph/0609522.
[27] A. W. Strong and I. V. Moskalenko, Astrophys. J. **509**, 212 (1998).
[28] C. Evoli, D. Gaggero, D. Grasso, and L. Maccione, J. Cosmol. Astropart. Phys. 10 (2008) 018.
[29] A. Putze, L. Derome, D. Maurin, L. Perotto, and R. Taillet, Astron. Astrophys. **497**, 991 (2009).
[30] A. Putze, L. Derome, and D. Maurin, Astron. Astrophys. **516**, A66 (2010).
[31] R. Trotta, G. Jóhannesson, I. V. Moskalenko, T. A. Porter, R. Ruiz de Austri, and A. W. Strong, Astrophys. J. **729**, 106 (2011).
[32] T. Sjöstrand, S. Mrenna, and P. Skands, J. High Energy Phys. 5 (2006) 026.
[33] S. Profumo, Eur. J. Phys. **10**, 1 (2011).
[34] D. Hooper, A. Stebbins, and K. M. Zurek, Phys. Rev. D **79**, 103513 (2009).
[35] M. Kuhlen and D. Malyshev, Phys. Rev. D **79**, 123517 (2009).
[36] D. Malyshev, I. Cholis, and J. Gelfand, Phys. Rev. D **80**, 063005 (2009).
[37] A. W. Strong, I. V. Moskalenko, and V. S. Ptuskin, Annu. Rev. Nucl. Part. Sci. **57**, 285 (2007).
[38] D. Maurin, F. Donato, R. Taillet, and P. Salati, Astrophys. J. **555**, 585 (2001).
[39] M. Pato, D. Hooper, and M. Simet, J. Cosmol. Astropart. Phys. 6 (2010) 022.
[40] D. Maurin, A. Putze, and L. Derome, Astron. Astrophys. **516**, A67 (2010).
[41] H. S. Ahn, P. Allison, M. G. Bagliesi, J. J. Beatty, G. Bigongiari, J. T. Childers, N. B. Conklin, S. Coutu, M. A. DuVernois, O. Ganel *et al.*, Astrophys. J. Lett. **714**, L89 (2010).
[42] O. Adriani, G. C. Barbarino, G. A. Bazilevskaya, R. Bellotti, M. Boezio, E. A. Bogomolov, L. Bonechi, M. Bongi, V. Bonvicini, S. Borisov *et al.*, Science **332**, 69 (2011).
[43] Y. Ohira and K. Ioka, Astrophys. J. Lett. **729**, L13 (2011).
[44] Q. Yuan, B. Zhang, and X.-J. Bi, Phys. Rev. D **84**, 043002 (2011).
[45] A. Lewis and S. Bridle, Phys. Rev. D **66**, 103511 (2002).
[46] M. A. Malkov and L. O'C Drury, Rep. Prog. Phys. **64**, 429 (2001).
[47] L. J. Gleeson and W. I. Axford, Astrophys. J. **154**, 1011 (1968).
[48] L. Zhang and K. S. Cheng, Astron. Astrophys. **368**, 1063 (2001).
[49] D. R. Lorimer, in *Young Neutron Stars and Their Environments*, IAU Symposium / Symp-Int.Astron.Union Vol. 218, edited by F. Camilo and B. M. Gaensler (Astronomical Society of the Pacific, Orem, Utah, 2004), p. 105.
[50] L. Bergström, J. Edsjö, and G. Zaharijas, Phys. Rev. Lett. **103**, 031103 (2009).
[51] I. Cholis, G. Dobler, D. P. Finkbeiner, L. Goodenough, and N. Weiner, Phys. Rev. D **80**, 123518 (2009).
[52] J. Einasto, Trudy Inst. Astrofiz. Alma-Ata **51**, 87 (1965).
[53] J. F. Navarro, A. Ludlow, V. Springel, J. Wang, M. Vogelsberger, S. D. M. White, A. Jenkins, C. S. Frenk, and A. Helmi, Mon. Not. R. Astron. Soc. **402**, 21 (2010).
[54] R. Catena and P. Ullio, J. Cosmol. Astropart. Phys. 8 (2010) 004.
[55] M. Pato, O. Agertz, G. Bertone, B. Moore, and R. Teyssier, Phys. Rev. D **82**, 023531 (2010).
[56] P. Salucci, F. Nesti, G. Gentile, and C. Frigerio Martins, Astron. Astrophys. **523**, A83 (2010).
[57] J. M. Clem, D. P. Clements, J. Esposito, P. Evenson, D. Huber, J. L'Heureux, P. Meyer, and C. Constantin, Astrophys. J. **464**, 507 (1996).
[58] G. Di Bernardo, C. Evoli, D. Gaggero, D. Grasso, L. Maccione, and M. N. Mazziotta, Astropart. Phys. **34**, 528 (2011).
[59] B. Beischer, P. von Doetinchem, H. Gast, T. Kirn, and S. Schael, New J. Phys. **11**, 105021 (2009).
[60] P. Bobik, M. J. Boschini, C. Consolandi, S. Della Torre, M. Gervasi, D. Grandi, K. Kudela, S. Pensotti, and P. G. Rancoita, arXiv:1011.4843.
[61] A. W. Strong, I. V. Moskalenko, and O. Reimer, Astrophys. J. **613**, 962 (2004).
[62] T. Kamae, N. Karlsson, T. Mizuno, T. Abe, and T. Koi, Astrophys. J. **647**, 692 (2006).
[63] G. D. Badhwar, R. L. Golden, and S. A. Stephens, Phys. Rev. D **15**, 820 (1977).
[64] V. Barger, Y. Gao, W. Y. Keung, D. Marfatia, and G. Shaughnessy, Phys. Lett. B **678**, 283 (2009).
[65] D. Chowdhury, C. J. Jog, and S. K. Vempati, Pramana **76**, 1 (2011).
[66] M. Pohl, Phys. Rev. D **79**, 041301 (2009).
[67] M. Pato, M. Lattanzi, and G. Bertone, J. Cosmol. Astropart. Phys. 12 (2010) 020.
[68] I. Cernuda, Astropart. Phys. **34**, 59 (2010).
[69] J. Zhang, X. J. Bi, J. Liu, S. M. Liu, P. F. Yin, Q. Yuan, and S. H. Zhu, Phys. Rev. D **80**, 023007 (2009).
[70] I. V. Moskalenko, A. W. Strong, J. F. Ormes, and M. S. Potgieter, Astrophys. J. **565**, 280 (2002).
[71] I. V. Moskalenko, A. W. Strong, S. G. Mashnik, and J. F. Ormes, Astrophys. J. **586**, 1050 (2003).
[72] F. Donato, D. Maurin, P. Salati, A. Barrau, G. Boudoul, and R. Taillet, Astrophys. J. **563**, 172 (2001).
[73] G. di Bernardo, C. Evoli, D. Gaggero, D. Grasso, and L. Maccione, Astropart. Phys. **34**, 274 (2010).
[74] J.-M. Zheng, Z.-H. Yu, J.-W. Shao, X.-J. Bi, Z. Li, and H.-H. Zhang, Nucl. Phys. **B854**, 350 (2012).
[75] J. Alcaraz, B. Alpat, G. Ambrosi, H. Anderhub, L. Ao, A. Arefiev, P. Azzarello, E. Babucci, L. Baldini, M. Basile *et al.*, Phys. Lett. B **490**, 27 (2000).
[76] T. Sanuki, M. Motoki, H. Matsumoto, E. S. Seo, J. Z. Wang, K. Abe, K. Anraku, Y. Asaoka, M. Fujikawa, M. Imori *et al.*, Astrophys. J. **545**, 1135 (2000).
[77] A. D. Panov, J. H. Adams, Jr., H. S. Ahn, K. E. Batkov, G. L. Bashindzhagyan, J. W. Watts, J. P. Wefel, J. Wu, O. Ganel, T. G. Guzik *et al.*, Bull. Russ. Acad. Sci. Phys. **71**, 494 (2007).
[78] M. Boezio, P. Carlson, T. Francke, N. Weber, M. Suffert, M. Hof, W. Menn, M. Simon, S. A. Stephens, R. Bellotti *et al.*, Astrophys. J. **518**, 457 (1999).

[79] M. Aguilar, J. Alcaraz, J. Allaby, B. Alpat, G. Ambrosi, H. Anderhub, L. Ao, A. Arefiev, P. Azzarello, L. Baldini *et al.*, Phys. Lett. B **646**, 145 (2007).

[80] S. W. Barwick, J. J. Beatty, A. Bhattacharyya, C. R. Bower, C. J. Chaput, S. Coutu, G. A. de Nolfo, J. Knapp, D. M. Lowder, S. McKee *et al.*, Astrophys. J. Lett. **482**, L191 (1997).

[81] S. Coutu, A. S. Beach, J. J. Beatty, A. Bhattacharyya, C. Bower, M. A. Duvernois, A. Labrador, S. P. McKee, S. Minnick, D. Muller *et al.*, in *International Cosmic Ray Conference*, International Cosmic Ray Conference Vol. 5 (American Institute of Physics, New York, 2001), p. 1687.

[82] M. Aguilar, J. Alcaraz, J. Allaby, B. Alpat, G. Ambrosi, H. Anderhub, L. Ao, A. Arefiev, P. Azzarello, E. Babucci *et al.*, Phys. Rep. **366**, 331 (2002).

[83] Y. Asaoka, Y. Shikaze, K. Abe, K. Anraku, M. Fujikawa, H. Fuke, S. Haino, M. Imori, K. Izumi, T. Maeno *et al.*, Phys. Rev. Lett. **88**, 051101 (2002).

[84] S. Haino, K. Abe, H. Fuke, T. Maeno, Y. Makida, H. Matsumoto, J. W. Mitchell, A. A. Moiseev, J. Nishimura, M. Nozaki *et al.*, in *International Cosmic Ray Conference*, International Cosmic Ray Conference Vol. 3 (American Institute of Physics, New York, 2005), pp. 13–+.

[85] D. S. Akerib, M. S. Armel-Funkhouser, M. J. Attisha, C. N. Bailey, L. Baudis, D. A. Bauer, P. L. Brink, P. P. Brusov, R. Bunker, B. Cabrera *et al.*, Phys. Rev. D **73**, 011102 (2006).

[86] J. Angle, E. Aprile, F. Arneodo, L. Baudis, A. Bernstein, A. Bolozdynya, L. C. C. Coelho, C. E. Dahl, L. Deviveiros, A. D. Ferella *et al.*, Phys. Rev. Lett. **101**, 091301 (2008).